

## Research



**Cite this article:** Iijima M, Qiao Y, Lin W, Peng Y, Yoneda M, Liu J. 2022 An intermediate crocodylian linking two extant gharials from the Bronze Age of China and its human-induced extinction. *Proc. R. Soc. B* **289**: 20220085.  
<https://doi.org/10.1098/rspb.2022.0085>

Received: 15 January 2022

Accepted: 4 February 2022

**Subject Category:**

Palaeobiology

**Subject Areas:**

evolution, palaeontology, taxonomy and systematics

**Keywords:**

phylogeny, crocodylia, acoustics, sexual selection, extinction, Holocene

**Author for correspondence:**

Jun Liu

e-mail: [junliu@hfut.edu.cn](mailto:junliu@hfut.edu.cn)

Electronic supplementary material is available online at <https://doi.org/10.6084/m9.figshare.c.5870758>.

# An intermediate crocodylian linking two extant gharials from the Bronze Age of China and its human-induced extinction

Masaya Iijima<sup>1,2,3</sup>, Yu Qiao<sup>1</sup>, Wenbin Lin<sup>4</sup>, Youjie Peng<sup>5</sup>, Minoru Yoneda<sup>6</sup> and Jun Liu<sup>1</sup>

<sup>1</sup>School of Resource and Environmental Engineering, Hefei University of Technology, 193 Tunxi Road, Baohe, Hefei, Anhui 230009, People's Republic of China

<sup>2</sup>Department of Biological Sciences, Clemson University, Clemson, SC 29634, USA

<sup>3</sup>Nagoya University Museum, Furocho, Chikusa-Ku, Nagoya, Aichi 464-8601, Japan

<sup>4</sup>Xinhui Museum, 12 Gongyuan Road, Xinhui, Jiangmen, Guangdong 529199, People's Republic of China

<sup>5</sup>Shunde Museum, Bishui Road, Shunde, Foshan, Guangdong 528300, People's Republic of China

<sup>6</sup>The University Museum, The University of Tokyo, Hongo 7-3-1, Bunkyo, Tokyo 113-0033, Japan

MI, 0000-0003-2701-0391; MY, 0000-0003-0129-8921; JL, 0000-0001-7859-5209

A solid phylogenetic framework is the basis of biological studies, yet higher level relationships are still unresolved in some major vertebrate lineages. One such group is Crocodylia, where the branching pattern of three major families (Alligatoridae, Crocodylidae and Gavialidae) has been disputed over decades due to the uncertain relationship of two slender-snouted lineages, gavialines and tomistomines. Here, we report a bizarre crocodylian from the Bronze Age of China, which shows a mosaic of gavialine and tomistomine features across the skeleton, rendering support to their sister taxon relationship as molecular works have consistently postulated. Gavialine characters of the new Chinese crocodylian include a novel configuration of the pterygoid bulla, a vocal structure known in mature male Indian gharials. Extinct gavialines have repeatedly evolved potentially male-only acoustic apparatus of various shapes, illuminating the deep history of sexual selection on acoustic signalling in a slender-snouted group of crocodylians. Lastly, a cutmark analysis combined with accelerator mass spectrometry (AMS) radiocarbon dating of bone remains demonstrated that two individuals from Shang and Zhou dynasties in Guangdong, China, suffered head injuries and decapitation. Archaeological evidence together with historical accounts suggests the human-induced extinction of this unique crocodylian only a few hundred years ago.

## 1. Introduction

Extant crocodylians are large semi-aquatic predators represented by approximately 30 species in the tropics and subtropics [1]. Many of the living species are currently under threat of extinction [2,3], yet few others experienced population recovery in recent decades [4–6]. Despite the low taxonomic and morphological diversity of extant species, fossil crocodylians exhibit unprecedented craniodental and postcranial morphologies, such as duck-like and extremely long snouts, ziphodont teeth and hoof-like unguals [7,8]. Moreover, morphometric analyses demonstrated that fossil species took currently unoccupied regions of skeletal morphospace, and crown group crocodylians underwent multiple disparity peaks during the Cenozoic [9–11].

Gavialoidea is a group of slender-snouted crocodylians including the living ecomorphological end-member, the Indian gharial (*Gavialis gangeticus*), which is characterized by a slender snout and short limbs [10,12]. Although this group is of importance to understand the evolutionary process of snout shape and associated skeletal morphologies [7,13], the clade position and membership, and relationships among clade members are still disputed [14–17]. The

debate stems from the different phylogenetic positions of the Indian gharial in molecular and morphological trees—the Indian gharial is the extant sister taxon to the Malayan gharial (*Tomistoma schlegelii*) in molecular trees [18–22], whereas it is an outgroup to all other extant crocodylians in morphological trees [16,23–26], except few recent ones that are consistent with the molecular tree [17,27]. Contrasting phylogenetic hypotheses based on molecular and morphological data confounded interpretation of cranial and postcranial evolution in crocodylians [10,14,15]. Although improved analytical protocols are required, the most important key to resolving the molecular–morphological phylogenetic conflict is sampling of new fossil taxa [16,19].

Here, we report a new, exceptionally well preserved crocodylian from the Bronze Age of southern China. Although the new Chinese crocodylian superficially resembles tomistomines, it shows a wealth of gavialine features including a potentially sexually selected vocal structure, reducing the morphological gap between gavialines and tomistomines and providing insights into sexual selection on acoustic signalling in crocodylians. It also represents one of the most compelling examples of the human-mediated reptile extinction in the late Quaternary. Chop marks left on the skeletons of two Bronze-age specimens together with historical accounts suggest that the human–crocodylian conflict had lasted in southern China from the Bronze Age until a few hundred years ago when this unique species finally became extinct.

## 2. Methods

### (a) Body length estimation

Snout–vent length (SVL) and total length (TL) of the holotype (XM 12-1558) and a paratype (SM E1623) of *Hanyusuchus sinensis* gen. et sp. nov. were estimated from the sum of the presacral centrum lengths and the sum of the cervical centrum lengths, respectively, using the equations in Iijima and Kubo [28]. Body lengths of the remaining paratypes without postcrania (XM 12-1557 and SM S01812) were estimated based on the skull–body length proportions in the holotype.

### (b) Accelerator mass spectrometry radiocarbon dating of bones

Lower jaw and rib fragments in the holotype (XM 12-1558) and paratypes (XM 12-1557; SM E1623) of *H. sinensis* were used for the dating. Collagen was extracted from the organic remains and purified using the gelatinization method [29]. Weight percentages and stable isotope ratios of carbon and nitrogen were measured using the Thermo Fisher Scientifics EA-IRMS system and compared with standard materials for calibration [30,31]. Following the routine CO<sub>2</sub> trapping and graphitization [32], the <sup>14</sup>C/<sup>12</sup>C ratio of graphite was measured with the AMS system in the Laboratory of Radiocarbon Dating, The University of Tokyo, Japan.  $\delta^{13}\text{C}$  measured in conjunction with the <sup>14</sup>C analysis was used for the isotopic fractionation correction [33]. Calibration of radiocarbon age determinations was done using the IntCal20 curve [34] in OxCal v. 4.2 [35]. Calibrated ages (in cal BP) were reported with 1-sigma error.

### (c) Cutmark analysis

A paratype skull (XM 12-1557) of *H. sinensis* preserves over a dozen chop marks on the skull table and the occipital condyle. Orientations of chop marks on the skull table with respect to the mediolateral axis of the skull were measured based on a

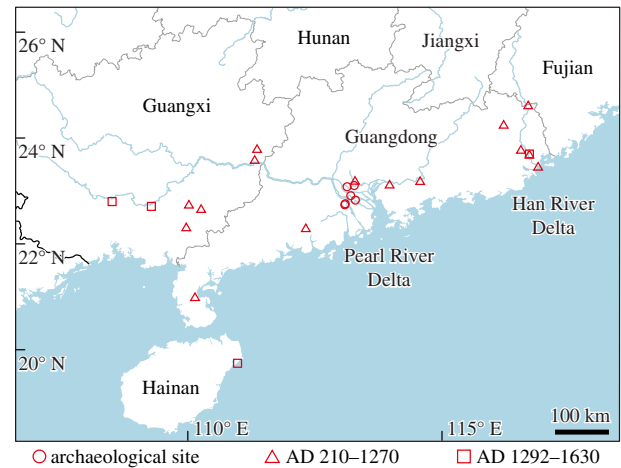


**Figure 1.** Historical distribution of *Hanyusuchus sinensis*, gen. et sp. nov. in Southern China (electronic supplementary material, figure S1 and tables S1 and S2 for details). (Online version in colour.)

photo image. A rose diagram was generated for showing the distribution of chop mark orientations. Biaxial orientation data were converted to unimodal circular data ( $0-2\pi$  radians), using the equation  $\alpha_{\text{adj}} = 2\alpha \pmod{2\pi}$ , where  $\alpha$  and  $\alpha_{\text{adj}}$  are original and adjusted orientations in radian, respectively [36]. Uniformity of orientation distribution was examined with the Rayleigh test, using the R package circular [37,38]. For enhanced visualization and measurements, silicon moulds of selected cutmarks were scanned using the Olympus LEXT OLS 4100 confocal laser microscope in the Light Imaging Facility, Clemson University, USA. Captured surface images were inverted in the operating software to match the real cutmark contour, and measurements were taken digitally.

### (d) Phylogenetic analyses

To assess the phylogenetic relationship of *H. sinensis*, we performed Bayesian and maximum-parsimony analyses using the revised data matrix (77 taxa and 254 discrete morphological characters) of Iijima and Kobayashi [15], which was largely based on earlier works (e.g. refs. [23,25,26,39]). Analyses were conducted with and without a backbone topological constraint of extant and subfossil taxa based on a molecular tree [22]. *Bernissartia fagesii* was designated as an outgroup and 15 characters were ordered. Bayesian analyses were executed in MrBayes v. 3.2.7 [40]. Markov chain Monte Carlo analyses were run with four chains in each of the two runs for 10 million generations, sampling every 10 000 generations, which resulted in 1000 samples per run. Maximum-parsimony analyses were executed in TNT v. 1.5 [41,42] without or with extended implied weighting ( $k = 3$  or 12). Heuristic searches were run with 10 000 random-addition-sequence replicates. See electronic supplementary material, part III for extended methodology of phylogenetic analyses.

## 3. Results

### (a) Systematics

Crocodylia Gmelin, 1789 (*sensu* Benton and Clark, 1988 (ref. [43])).

Gavialidae Adams, 1854 (*sensu* Brochu, 2003 (ref. [44]), molecular context).

*Hanyusuchus sinensis* gen. et sp. nov.

### (i) Etymology

The generic name after Han Yu (a Chinese government official and poet during the Tang dynasty) + suchus (Latin for

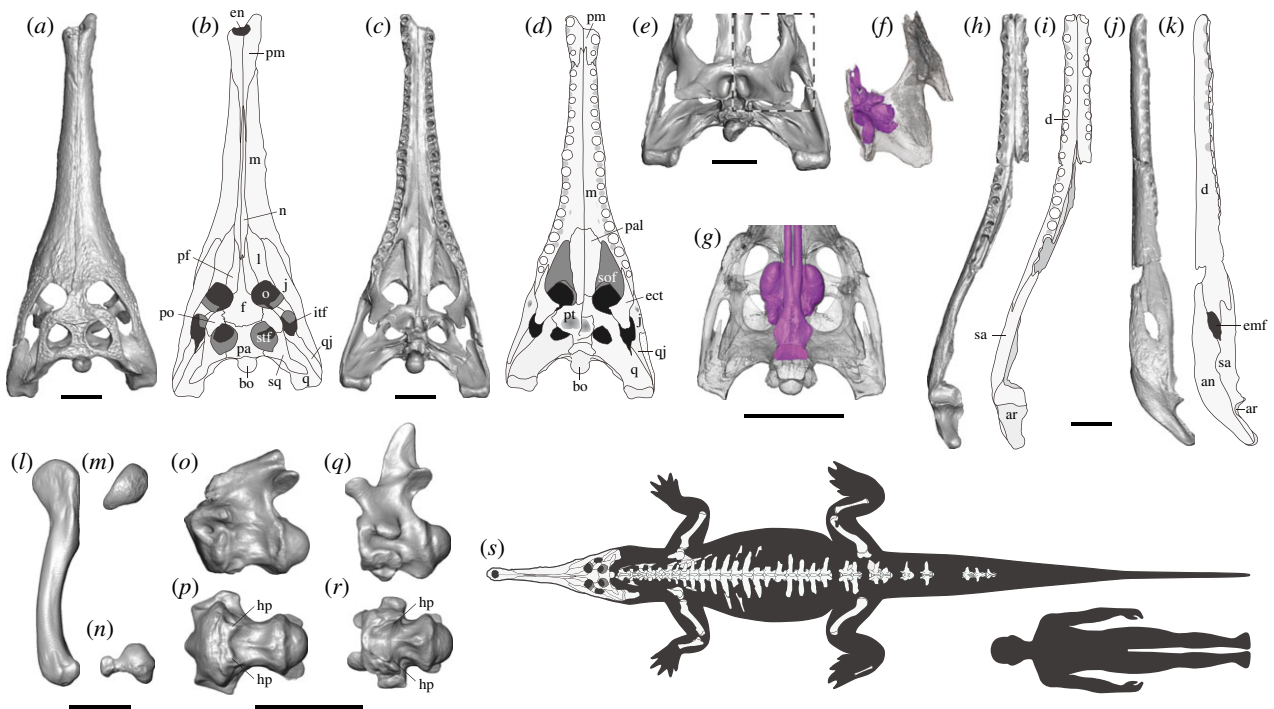


**Figure 2.** Anatomy of *Hanyusuchus sinensis*, gen. et sp. nov. from the Bronze Age of southern China. (a–d) Holotype skull (XM 12-1558) in dorsal (a,b) and ventral (c,d) views. (e) Posterior skull of a paratype (XM 12-1557) in ventral view. (f) Three-dimensional reconstruction of the boxed part in (e), highlighting the pterygoid bulla (purple volume). (g) Three-dimensional reconstruction of the pterygoid bullae and nasopharyngeal duct (purple volume) in *Gavialis gangeticus* (UF 118998). (h–k) Holotype mandible (XM 12-1558) in dorsal (h,i) and left lateral (j,k) views. (l–n) Left femur of the holotype (XM 12-1558) in lateral (l), proximal (m) and distal (n) views. (o,p) Axis of a paratype (SM E1623) in left lateral (o) and ventral (p) views. (q,r) Third cervical vertebra of the holotype (XM 12-1558) in left lateral (q) and ventral (r) views. (s) Composite reconstruction of *H. sinensis* scaled to the holotype (XM 12-1558) compared with a human (1.8 m height). an, angular; ar, articular; bo, basioccipital; d, dentary; ect, ectopterygoid; emf, external mandibular fenestra; en, external naris; f, frontal; hp, hypapophysis; itf, infratemporal fenestra; j, jugal; l, lacrimal; m, maxilla; n, nasal; o, orbit; pa, parietal; pal, palatine; pf, prefrontal; pm, premaxilla; po, postorbital; pt, pterygoid; q, quadrate; qj, quadratojugal; sa, surangular; sof, soborbital fenestra; sq, squamosal; stf, supratemporal fenestra. Scale bars are 10 cm. (Online version in colour.)

Greek *soûkhos*, the crocodile god Sobek), and the specific epithet after *sinae* (Latin for China) + *ensis* (Latin for ‘from’).

### (ii) Holotype

XM 12-1558, skull, lower jaw and partial postcrania from Dalincun, Tangxiazhen, Pengjiang District, Jiangmen, Guangdong Province (3327 ± 53 cal BP (1 s.d.)) (electronic supplementary material, figure S1).

### (iii) Paratypes

XM 12-1557, skull from Shitoucun, Tangxiazhen, Pengjiang District, Jiangmen, Guangdong Province (3297 ± 48 cal BP (1 s.d.)); SM E1623, skull, lower jaw and partial postcrania from Longyancun, Leiliuzhen, Shunde District, Foshan, Guangdong Province (2942 ± 55 cal BP (1 s.d.)); SM S01812, skull from Sijicun, Ronggui, Shunde District, Foshan, Guangdong Province (radiocarbon age unknown) (electronic supplementary material, figure S1).

### (iv) Distribution

Archaeological records and historical literature revealed the past occurrences of *H. sinensis* across Fujian, Guangdong, Guangxi, and Hainan provinces in southeastern China from the late fourth millennium BC to the mid second millennium AD (figure 1; electronic supplementary material, figure S1 and tables S1 and S2).

### (v) Diagnosis

A large slender-snouted crocodylian with five premaxillary, 16 maxillary and 18 dentary teeth; seventh maxillary tooth largest in the anterior-mid maxilla; medial wall of the last three maxillary alveoli within the suborbital fenestrae swollen; dorsal half of the prefrontal pillar narrow anteroposteriorly, and the medial process of the pillar dorsoventrally tall and anteroposteriorly short; interfenestral bar wider than one half of the interorbital distance; postorbital and squamosal parts of the skull table slope laterally; a shallow fossa extending posteriorly from the supratemporal fenestra onto the dorsal squamosal surface (autapomorphy); a pair of deep depressions anterior to the internal choana associated with the expansion of the posterior chamber of the pterygoid bulla; exoccipital sending a robust process ventrally to the basioccipital tubera; a pair of knob-like hypapophyses on the ventral surface of axial and third cervical centra; anterior margin of dorsal midline osteoderms with anterior process; reduced medial condyle of the femur (figure 2a–r; see electronic supplementary material, part I and II and figures S2–S21 for full description and comparisons, and electronic supplementary material, tables S3–S5 for measurements).

### (vi) Maturity and body size

The holotype (XM 12-1558) and a paratype (SM E1623) show closed neurocentral sutures in precaudal vertebrae, indicating sexual maturity [28,45,46], although their sexes are unknown. Body length (SVL and TL) estimates are 2.83 m SVL and 5.43 m TL for XM 12-1558 (figure 2s), 3.23 m SVL and

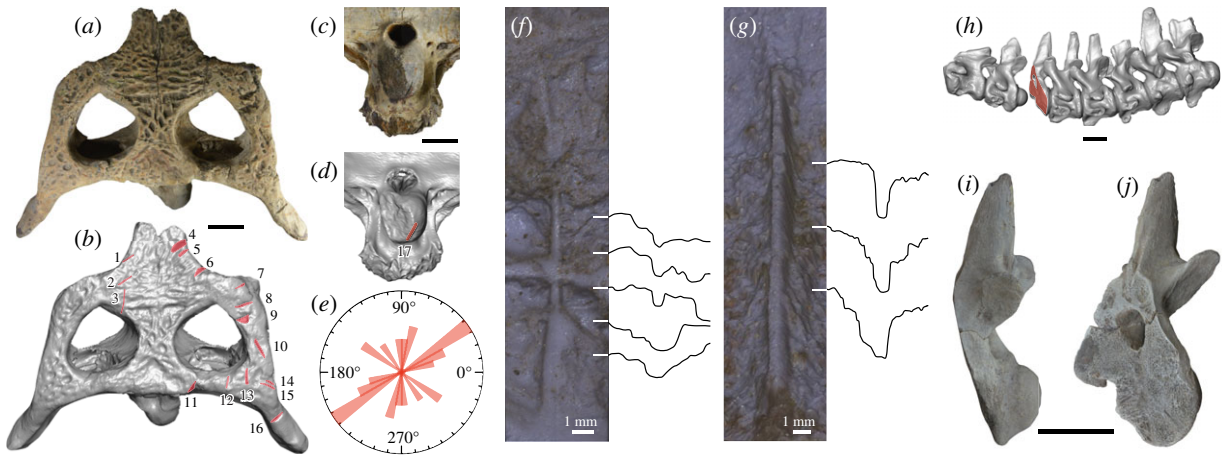


**Figure 3.** Chop marks left on *Hanyusuchus sinensis*, gen. et sp. nov. from the Bronze Age of southern China. (a–d) Seventeen chop marks on the skull table to periorbital region (a,b) and the occipital condyle (c,d) in a paratype (XM 12-1557). (e) Orientations of chop marks on the skull table with respect to the mediolateral axis of a paratype skull (XM 12-1557). (f,g) Close-up of chop marks no. 3 (f) and no. 17 (g) in a paratype skull (XM 12-1557). (h) Cervical vertebrae in a paratype (SM E1623) highlighting the cut surface of the fourth cervical vertebra. (i,j) Posterior half of the bisected fourth cervical vertebra in a paratype (SM E1623) in lateral (i) and anterolateral (j) views. Scale bars for a–d, h–j are 5 cm. (Online version in colour.)

6.19 m TL for XM 12-1557, 2.88 m SVL and 5.57 m TL for SM E1623 and 3.09 m SVL and 5.97 m TL for SM S01812.

### (b) Cutmarks

Seventeen chop marks, 16 on the skull table to periorbital region and one on the occipital condyle were found in a paratype (XM 12-1557: figure 3a–d; electronic supplementary material, figure S22). Chop marks on the skull table to periorbital region are mostly distributed on its right side. Although some chop marks show similar orientations, the Rayleigh test did not reject uniform distribution of chop mark orientations ( $z = 2.181$ ,  $p = 0.112$ ) (figure 3e). All the chop marks have straight or nearly straight edges. Vertical chop marks (no. 1–3, 7, and 17) are narrow and deep, showing the smooth floor. The two longest vertical chop marks on the anterior skull table (no. 3) and occipital condyle (no. 17) are 16.3 mm and 19.2 mm in length, respectively. Their maximum depths and breadths where both cutting edges are clearly defined are 0.7 mm and 0.6 mm, respectively in no. 3 and 3.2 mm and 0.8 mm, respectively in no. 17 (figure 3f,g). Obliquely angled chop marks (no. 4–6 and 8–16) often have a smooth and flat kerf wall and an irregularly fractured wall on the other side that are characteristics of metal chop marks [47,48]. The kerf wall widths measured perpendicular to the bottom grooves are approximately 6–7 mm for no. 4, 10 and 11. Similar orientations of closely spaced chop marks (no. 4–9) indicate multiple chops by the same person. Because the smooth kerf walls of these chop marks face posterodorsally, a right-handed person might chop the skull from its right side. Chop marks oriented in different directions (no. 3 and 10–13) could be made by the same person from different positions or by other people. A prominent chop mark was also found in the fourth cervical vertebra of a different paratype (SM E1623: figure 3h–j; electronic supplementary material, figure S23), as briefly mentioned by Zeng [49]. The entire vertebra was bisected obliquely in a single blow. The cut surface (110 mm height and 79 mm width) is flat and clean, exposing the cancellous bone tissues. The cutting edge is sharp and clearly defined on the left side and slightly fractured on the right side, suggesting the chopping from the left to right side.

### (c) Phylogenetic analyses

A 50% majority rule consensus tree from the Bayesian analysis with a topological constraint of extant and subfossil taxa based on the molecular hypothesis is shown in figure 4 (also see electronic supplementary material, figure S24a). The constrained Bayesian tree recovered the clade of *Penghusuchus pani*, *Toyotamaphimeia machikanensis* and *H. sinensis* as sister to *Eosuchus* and more derived gavialines as in constrained parsimonious trees (electronic supplementary material, figure S25 and table S6). The unconstrained Bayesian tree recovered Alligatoroidea as an outgroup of Gavialoidea + Crocodyloidea (electronic supplementary material, figure S24b), unlike the unconstrained parsimonious trees that recovered Alligatoroidea as sister to Crocodyloidea (electronic supplementary material, part IV, figure S26 and table S6).

## 4. Discussion

### (a) A new Chinese crocodylian as a key taxon to resolving the molecular–morphological phylogenetic conflict

*H. sinensis* is an intermediate taxon that reduces the morphological gap between two lineages leading to Indian and Malayan gharials (gavialines and tomistomines in the molecular context: ref. [44]). Previously, two extant gharials were either distantly placed in the majority of the morphological trees ([14,23,26]; but see [17,27] that indicated otherwise) or formed an extant sister group in molecular or combined morphological + molecular trees [14,15,19,60]. Recent work demonstrated the presence of gavialine features in post-Palaeogene crocodylians from East Asia (*P. pani* and *T. machikanensis*) that were previously considered as tomistomines, rendering support for the molecular tree [15]. Despite the superficial resemblance to tomistomines, *H. sinensis* shares many of those gavialine features, such as (i) exoccipital sending a robust and anteroposteriorly wide descending process to the basioccipital tubera (electronic supplementary material, figure S7); (ii) splenial symphysis wide V-shape in dorsal view (figure 2h,i); (iii) forked axial hypapophyses

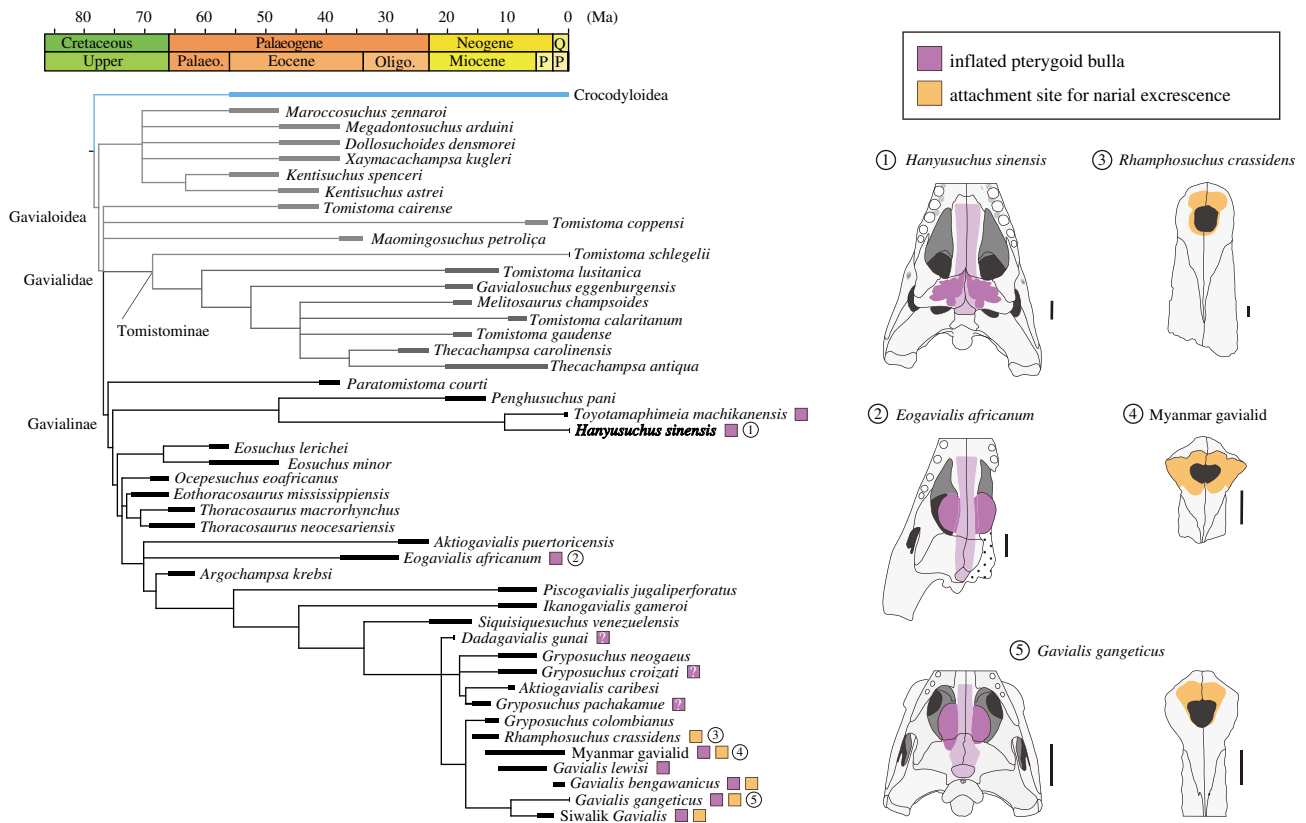


**Figure 4.** Gavialoid phylogeny and the evolution of the acoustic apparatus. Phylogenetic relationships were obtained from Bayesian analysis with a backbone constraint of extant and subfossil taxa based on a molecular tree [22]. Shared branch lengths were divided equally using the R package palaeotree [38,50], and branch colours correspond to those in figure 5. Phylogenetic distribution of the inflated pterygoid bulla and the attachment site for the narial excrescence are based on first-hand observation and literature [51–59]. Illustration source: *Eogavialis africanum* (Senckenberg Museum specimen [56]; pathway of the nasopharyngeal duct estimated); *G. gangeticus* (BMNH 2005.1601; UF 118998); *Hanyusuchus sinensis* (XM 12-1557; XM 12-1558); Myanmar gavialid (MZKB F1160) and *Rhamphosuchus crassidens* (BMNH 39802). All scale bars are 5 cm. (Online version in colour.)

(figure 2*p*); (iv) absence of keel-like hypapophysis in the third cervical vertebra (figure 2*r*); (v) inter-zygapophyseal widths narrow in dorsal vertebrae (electronic supplementary material, figures S13 and S14) and (vi) dorsal or pelvic midline osteoderms bearing anterior process (electronic supplementary material, figure S21).

Exquisite preservation of *H. sinensis* allowed observation of many more gavialine features. The dorsal half of the prefrontal pillar is narrow anteroposteriorly, and the medial process is dorsoventrally tall and anteroposteriorly short in *H. sinensis* (XM 12-1558; SM S01812; electronic supplementary material, figure S8*c–f*), resembling stem and basal crocodylians and gavialines [61,62]. The postorbital and squamosal parts of the skull table slope laterally in *H. sinensis* (XM 12-1557; XM 12-1558; SM S01812; electronic supplementary material, figure S2*c,f,i*) as in stem crocodylians, gavialines and a few tomistomines [62,63]. The lateral sloping of the skull table in *H. sinensis* is moderate compared with that in gavialines, but the sloping is obvious in occipital view. Additionally, the medial condyle of the femur is reduced and considerably smaller than the lateral condyle in distal view in *H. sinensis* (XM 12-1558; figure 2*n*), which is shared with *G. gangeticus* (AMNH 88316; UF 70592; UF 118998) and *G. bengawanicus* [51]. In other gavialoids including *Eosuchus minor* (USNM 355967) and *Maomingosuchus petrolica* (IVPP V5015), anteroposterior lengths of the medial and lateral condyles are subequal, or the medial condyle is only slightly shorter than the lateral one in distal view.

Although our phylogenetic trees without a topological constraint are overall consistent with previous morphological trees, those with a constraint on extant and subfossil taxa placed post-Palaeogene crocodylians from East Asia (*P. pani*, *T. machikanensis* and *H. sinensis*) at basal Gavialinae near the split of gavialines and tomistomines (figure 4). A mosaic of gavialine and tomistomine features in these East Asian taxa explains their basal gavialine status in constrained morphological trees [15,17]. A phylomorphospace based on the cladistic character dataset corroborates the notion that three East Asian crocodylians are intermediate taxa linking gavialines and non-gavialine gavialoids (figure 5; see electronic supplementary material, part III for methodology). These East Asian taxa occupy the edge of gavialine morphospace and are partially overlapped with non-gavialine gavialoids.

### (b) Implication for sexual selection on acoustic signalling in crocodylians

*H. sinensis* exhibits a cranial feature that is relevant to acoustic function unique to mature male Indian gharials. Multiple sinuses that occupy the pterygoid in *H. sinensis* (figure 2*f*; electronic supplementary material, figure S6*c*) would be homologous to the posterior chamber of the pterygoid bulla, which is confined to the anterior part of the pterygoid in the Indian gharial (figure 2*g*; refs. [52,64]). Although the dorsal surface of the palatine is broken in *H. sinensis*, it might also have the anterior chamber of the pterygoid bulla

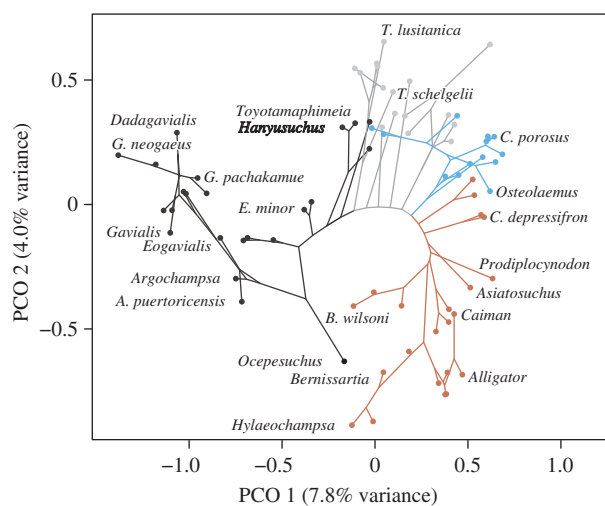


**Figure 5.** Phylomorphospace based on the principal coordinate analysis of the morphological distance matrix converted from the cladistic character dataset (77 taxa and 254 characters) and the constrained Bayesian tree. Branch colours are black for Gavialinae, grey for non-gavialine gavialoids, blue for Crocodyloidea and brown for non-Longirostres crocodylians (figure 4; electronic supplementary material, figure S24a). (Online version in colour.)

as in the Indian gharial. The anterior and posterior chambers of the pterygoid bulla, the closed-end chambers, are connected to the nasopharyngeal duct and would change harmonics of the sound, depending on the chamber lengths [52]. In the Indian gharial, inflation of the bulla during ontogeny is coupled with development of the narial excrescence, a soft tissue surrounding the osteological external naris, which houses the dorsoposterior extension of the nasal cavity [52]. Elongation of the nasal cavity would reduce dispersion of formant, the resonance frequency of the vocal tract—the hypothesis supported by change in formant frequencies yet near constant fundamental frequencies of the source signal during the experimental alteration of vocal tract lengths in Chinese alligators [65] and through ontogeny in American alligators [66]. Because vocal tract lengths are physically constrained and correlated with body size in many mammals and birds and a few crocodylians examined thus far, formants were considered as honest cues of body size for intraspecific communication in those taxa [66–68]. The narial excrescence that elongates the vocal tract likely evolved to exaggerate size in the Indian gharial, which would be functionally analogous to the cranial crest enclosing the elongated nasal cavity in lambeosaurine hadrosaurs [69] and the elongated trachea in some birds [70]. Presumably, the cost of vocal tract elongation (e.g. increased drag during underwater head sweeping) was smaller than the advantage of size exaggeration in male Indian gharials.

Potential evidence of sexual selection on the acoustic size exaggerator (narial excrescence) and sound modifier (pterygoid bulla) has been known in extinct gavialoids (figure 4). Perinarial depressions in ‘tomistomines’ *Rhamphosuchus crassidens* and ‘Gavialis’ *pachyrhynchus* [52,53,71] and a pair of rugose-tipped protuberances on both sides of the naris in a Myanmar gavialid and *G. bengawanicus* [51,54] were considered as the attachment sites for the narial excrescence. Additionally, the presence of the inflated anterior chamber of the pterygoid bulla was confirmed in *Eogavialis africanum*, *G. lewisi* and *G. bengawanicus* [51,55,56,72] and suggested in *Dadagavialis gunai*, *Gryposuchus croizati* and *G. pachakamue*

[57–59]. Furthermore, *H. sinensis* shows a novel expansion of the posterior chamber of the bulla, increasing the bulla morphological diversity. The expanded posterior chamber of the bulla is associated with the development of a pair of deep depressions anterior to the internal choana in *H. sinensis* (XM 12-1557; XM 12-1558; SM S01812; electronic supplementary material, figure S6b). Similarly large anterior choanal depressions are known in *G. lewisi* [55,73], implying the existence of the expanded posterior chamber in this species.

Assuming that the narial excrescence and the inflated pterygoid bulla are mature male-only throughout the crocodylian evolution, our phylogenetic tree that was forced to fit the molecular hypothesis indicates the repeated evolution of sexually selected acoustic apparatus within Gavialinae, a slender-snouted group of crocodylians (figure 4). The Indian gharial and fossil gavialines with the possible narial excrescence are large to giant taxa [2,51,53,74], consistent with the acoustic size exaggeration hypothesis that posits selection for larger body size precedes sexual selection on the size exaggerator [70]. The function of modified harmonics through the pterygoid bulla is ambiguous, but its presence only in slender-snouted gavialines may suggest the auxiliary role in size deception, as selection for the longer snout, thus the longer vocal tract, augments acoustic size exaggeration. Conceivably, extinct gavialines might rely more on acoustic than visual size cues, as the extant gavialine Indian gharial does not use head oblique tail arched posture [75], an honest visual body size signal [76].

### (c) Human-induced extinction of a large crocodylian in southern China

*H. sinensis* is of archaeological significance as it provides direct evidence of human–animal interaction in ancient China. Over a dozen of chop marks on the skull table to periorbital region in XM 12-1557 (figure 3a,b) imply an intention of killing this individual by inflicting wounds on the head, while a chop mark on the occipital condyle (figure 3c,d) might be the result of postmortem dismemberment. Similarly, a large chop mark on the fourth cervical vertebra in SM E1623 (figure 3h–j) could result from decapitation. Given the anterior inclination of the cut surface, the executor chopped down the neck of this individual diagonally in the left anterodorsal to right posteroventral direction, probably aiming at the gap between postoccipital and nuchal osteoderms. Decapitation of this large individual likely required multiple chops to sever soft tissues around the vertebra, although the bone appears to be bisected in a single blow.

The parallel-walled, deep vertical chop marks in the skull (XM 12-1557; figure 3f,g) and a large cut surface of the vertebra (SM E1623; figure 3i,j) support the use of heavy metal implements. Two chop mark bearing specimens from Guangdong are dated to Shang and Zhou dynasties (14–10th century BC) in the Chinese Bronze age, during which bronze axes were symbols of monarchical power and religious activities [77]. Although the appearance of bronze cultures in southeastern China lagged behind Yellow and Yangtze valley regions, multiple Shang dynasty culture sites in Guangdong yielded bronze tools, weapons, and casting moulds, indicating the presence of local bronze metallurgy [78–80]. These suggest that bronze weapons like axes as potential implements used for chopping the crocodylians.

Historical Chinese literature depicted human–crocodylian conflict in southeastern China from the early first to mid second millennium AD. The ancient Chinese crocodylian, most likely *H. sinensis*, was described as a huge aquatic animal with a long snout and sharp teeth, which often attacked people and livestock [81] (electronic supplementary material, table S1). To remove and exterminate crocodylians, government officials in Tang, Song and Ming dynasties (9–15th century AD) resorted to sacrificial rituals and forces in the Han River valley, eastern Guangdong [81,82] (electronic supplementary material, table S1). The ancient Cantonese hatred of crocodylians had lasted for at least three millennia since the Shang dynasty, as two chop mark bearing specimens from Shang and Zhou dynasties were discovered in the Pearl River delta, Guangdong.

The extinction of *H. sinensis* was supposedly caused by human-induced habitat degradation and loss, along with killing as evidenced by archaeological records and ancient literature. Historically, before the mid second millennium AD, *H. sinensis* was distributed along the major river systems across Guangxi, Guangdong and Fujian (figure 1; electronic supplementary material, figure S1). The range of *H. sinensis* would be progressively contracted during the past two millennia, as hotspots of the population associated with intensive agricultural activities emerged in southern China [83,84]. These population and agricultural dynamics appear to be closely tied to the range contraction and extirpation of Chinese mammalian megafauna (elephants, rhinoceroses, tigers and bears) [84]. Although climate changes also played roles in the megafauna extinction in China and other zoogeographical regions [85–87], it would not be the major driver of the demise of *H. sinensis*, because they survived until a few hundred years ago.

## References

- Grigg GC, Kirshner D. 2015 *Biology and evolution of crocodylians*. Clayton South, VIC, Australia: CSIRO Publishing.
- Stevenson C, Whitaker R. 2010 Indian gharial *Gavialis gangeticus*. In *Crocodyles. Status survey and conservation action plan*, 3rd edn (eds CS Manolis, C Stevenson), pp. 139–143. Darwin, NT, Australia: Crocodile Specialist Group.
- Thorbjarnarson JB, Wang X. 2010 *The Chinese alligator: ecology, behavior, conservation, and culture*. Baltimore, MD: The Johns Hopkins University Press.
- Webb GJW, Britton ARC, Manolis CS, Ottley B, Stirrat S. 2000 The recovery of *Crocodylus porosus* in the Northern Territory of Australia: 1971–1998. In *Crocodyles. Proc. 15th Working Meeting of the IUCN-SSC Crocodile Specialist Group* (ed. IUCN). Gland, Switzerland, pp. 195–234.
- Elsley RM, Woodward AR. 2010 American alligator *Alligator mississippiensis*. In *Crocodyles. Status survey and conservation action plan*, 3rd edn (eds CS Manolis, C Stevenson), pp. 1–4. Darwin, NT, Australia: Crocodile Specialist Group.
- Fukuda Y, Webb GJW, Manolis CS, Delaney R, Letnic M, Lindner G, Whitehead P. 2011 Recovery of saltwater crocodiles following unregulated hunting in tidal rivers of the Northern Territory, Australia. *J. Wildl. Manage.* **75**, 1253–1266. (doi:10.1002/jwmg.191)
- Brochu CA. 2001 Crocodylian snouts in space and time: phylogenetic approaches toward adaptive radiation. *Am. Zool.* **41**, 564–585. (doi:10.1668/0003-1569(2001)041[0564:CSISAT]2.0.CO;2)
- Brochu CA. 2013 Phylogenetic relationships of Palaeogene ziphodont eusuchians and the status of *Pristichampsus* Gervais, 1853. *Earth Env. Sci. Trans. R. Soc. Edinb.* **103**, 521–550. (doi:10.1017/S1755691013000200)
- Wilberg EW. 2017 Investigating patterns of crocodyliform cranial disparity through the Mesozoic and Cenozoic. *Zool. J. Linn. Soc.* **181**, 189–208. (doi:10.1093/zoolinnean/zlw027)
- Iijima M, Kubo T, Kobayashi Y. 2018 Comparative limb proportions reveal differential locomotor morphofunctions of alligatoroids and crocodyloids. *R. Soc. Open Sci.* **5**, 171774. (doi:10.1098/rsos.171774)
- Stubbs TL, Pierce SE, Elsler A, Anderson PSL, Rayfield EJ, Benton MJ. 2021 Ecological opportunity and the rise and fall of crocodylomorph evolutionary innovation. *Proc. R. Soc. B* **288**, 20210069. (doi:10.1098/rspb.2021.0069)
- Pierce SE, Angielczyk KD, Rayfield EJ. 2008 Patterns of morphospace occupation and mechanical performance in extant crocodylian skulls: a combined geometric morphometric and finite element modeling approach. *J. Morphol.* **269**, 840–864. (doi:10.1002/jmor.10627)
- Morris ZS, Vliet KA, Abzhanov A, Pierce SE. 2019 Heterochronic shifts and conserved embryonic shape underlie crocodylian craniofacial disparity and convergence. *Proc. R. Soc. B* **286**, 20182389. (doi:10.1098/rspb.2018.2389)
- Lee MSY, Yates AM. 2018 Tip-dating and homoplasy: reconciling the shallow molecular divergences of modern gharials with their long fossil record. *Proc. R. Soc. B* **285**, 20181071. (doi:10.1098/rspb.2018.1071)
- Iijima M, Kobayashi Y. 2019 Mosaic nature in the skeleton of East Asian crocodylians fills the morphological gap between ‘Tomistominae’ and Gavialinae. *Cladistics* **35**, 623–632. (doi:10.1111/clad.12372)
- Groh SS, Upchurch P, Barrett PM, Day JJ. 2020 The phylogenetic relationships of neosuchian crocodiles and their implications for the convergent evolution

**Data accessibility.** Data supporting the results of this study (full description of *H. sinensis*, morphological comparisons, extended methodology, results of maximum-parsimony analyses, supplementary figures and tables, MrBayes and TNT files used in the phylogenetic analyses, and data and codes used for generating phylogenetic morphospace) are provided in electronic supplementary material [88].

**Authors’ contributions.** M.I.: conceptualization, data curation, formal analysis, investigation, methodology, resources, validation, visualization, writing—original draft; Y.Q.: writing—review and editing; W.L.: resources; Y.P.: resources; M.Y.: investigation, writing—review and editing; J.L.: conceptualization, investigation, funding acquisition, project administration, supervision, writing—review and editing.

All authors gave final approval for publication and agreed to be held accountable for the work performed therein.

**Competing interests.** The authors declare no competing interests.

**Funding.** This study was supported by National Natural Science Foundation of China (grant nos. 42172026 and 41772003 to J.L., and 42002021 to M.I.); Fundamental Research Funds for the Central Universities of China (grant no. PA2020GDKC0022 to J.L.); Department of Natural Resources of Anhui Province (grant no. 2021-g-216 to J.L.); China Scholarship Council (grant no. 202106690044 to Y.Q.); and JSPS Grant-in-Aid for Scientific Research (grant nos. 19J00701 to M.I., and 15H05969 and 20H05821 to M.Y.).

**Acknowledgements.** We thank J. Jin and M. Tanimoto for providing information regarding *Hanyusuchus* collections in Guangdong, Q. Rao, Q. Li and J. Cui for helping cutmark moulding and surface and CT scanning, Z. Yang for allowing access to his  $\mu$ CT facility, M. Eda for his helpful comments on the cutmarks, Y. Kobayashi for providing CT data of *T. machikanensis*, H. Ozaki and T. Kubo for facilitating the radiocarbon dating and E. Hekkala for discussion. R. Blob, C. Brochu, T. Ikejiri, J. Ristevski and an anonymous reviewer provided helpful feedback that significantly improved the quality of the manuscript. The use of the confocal laser microscope was supported by Light Imaging Facility, Clemson University. CT data of an Indian gharial (UF 118998; MorphoSource media ID: 000039794) were courtesy of D. Blackburn, E. Stanley and C. Sheehy.

- of the longirostrine condition. *Zool. J. Linn. Soc.* **188**, 473–506. (doi:10.1093/zoolinnean/zlz117)
17. Rio J, Mannion P. 2021 Phylogenetic analysis of a new morphological dataset elucidates the evolutionary history of Crocodylia and resolves the long-standing gharial problem. *PeerJ* **9**, e12094. (doi:10.7717/peerj.12094)
  18. Densmore LD. 1983 Biochemical and immunological systematics of the order Crocodylia. In *Evolutionary biology* (eds MK Hechet, B Wallace, GH Prance), pp. 397–465. New York, NY: Plenum.
  19. Gatesy J, Amato GD, Norell MA, DeSalle R, Hayashi C. 2003 Combined support for wholesale taxic atavism in gavialine crocodylians. *Syst. Biol.* **52**, 403–422. (doi:10.1080/10635150350197037)
  20. Oaks JR. 2011 A time-calibrated species tree of Crocodylia reveals a recent radiation of the true crocodiles. *Evolution* **65**, 1–13. (doi:10.5061/dryad.5k9s0)
  21. Pan T *et al.* 2021 Near-complete phylogeny of extant Crocodylia (Reptilia) using mitogenome-based data. *Zool. J. Linn. Soc.* **191**, 1075–1089. (doi:10.1093/zoolinnean/zlaa074)
  22. Hekkala E *et al.* 2021 Paleogenomics illuminates the evolutionary history of the extinct Holocene ‘horned’ crocodile of Madagascar, *Voay robustus*. *Commun. Biol.* **4**, 505. (doi:10.1038/s42003-021-02017-0)
  23. Brochu CA. 1997 Morphology, fossils, divergence timing, and the phylogenetic relationships of *Gavialis*. *Syst. Biol.* **46**, 479–522. (doi:10.1093/sysbio/46.3.479)
  24. Brochu CA. 1999 Phylogenetics, taxonomy, and historical biogeography of Alligatoroidea. *J. Vertebr. Paleontol.* **19**, 9–100. (doi:10.1080/02724634.1999.10011201)
  25. Salisbury SW, Molnar RE, Frey E, Willis PMA. 2006 The origin of modern crocodyliforms: new evidence from the Cretaceous of Australia. *Proc. R. Soc. B* **273**, 2439–2448. (doi:10.1098/rspb.2006.3613)
  26. Jouve S, Bouya B, Amaghaz M, Meslouh S. 2015 *Maroccosuchus zennaroi* (Crocodylia: Tomistominae) from the Eocene of Morocco: phylogenetic and palaeobiogeographical implications of the basalmost tomistomine. *J. Syst. Palaeontol.* **13**, 421–445. (doi:10.1080/14772019.2014.913078)
  27. Ristevski J, Yates AM, Price GJ, Molnar RE, Weisbecker V, Salisbury SW. 2020 Australia’s prehistoric ‘swamp king’: revision of the Plio-Pleistocene crocodylian genus *Pallimnarchus* de Vis, 1886. *PeerJ* **8**, 1–98. (doi:10.7717/peerj.10466)
  28. Iijima M, Kubo T. 2020 Vertebrae-based body length estimation in crocodylians and its implication for sexual maturity and the maximum sizes. *Integr. Org. Biol.* **2**, obaa042. (doi:10.1093/iob/obaa042)
  29. Longin R. 1971 New method of collagen extraction for radiocarbon dating. *Nature* **230**, 241–242. (doi:10.1038/230241a0)
  30. DeNiro MJ. 1985 Postmortem preservation and alteration of *in vivo* bone collagen isotope ratios in relation to palaeodietary reconstruction. *Nature* **317**, 806–809. (doi:10.1038/317806a0)
  31. van Klinken GJ. 1999 Bone collagen quality indicators for palaeodietary and radiocarbon measurements. *J. Archaeol. Sci.* **26**, 687–695. (doi:10.1006/jasc.1998.0385)
  32. Omori T, Yamazaki K, Kabasawa T, Itahashi Y, Ozaki H, Yoneda M. 2017 High-precision radiocarbon dating of small-scale samples. In *Proc. 20th Japanese Symp. Accel. Mass Spectrom.*, p. 55.
  33. Stuiver M, Polach HA. 1977 Discussion: reporting of <sup>14</sup>C data. *Radiocarbon* **19**, 355–363. (doi:10.1017/S0033822200003672)
  34. Reimer PJ *et al.* 2020 The IntCal20 northern hemisphere radiocarbon age calibration curve (0–55 cal kBP). *Radiocarbon* **62**, 725–757. (doi:10.1017/RDC.2020.41)
  35. Ramsey CB. 2009 Bayesian analysis of radiocarbon dates. *Radiocarbon* **51**, 337–360. (doi:10.1017/s0033822200033865)
  36. Berens P. 2009 CircStat: a MATLAB toolbox for circular statistics. *J. Stat. Softw.* **31**, 1–21. (doi:10.18637/jss.v031.i10)
  37. Agostinelli C, Lund U. 2017 R package ‘circular’: circular statistics. R package version 0.4-93.
  38. R Core Team. 2020 *R: a language and environment for statistical computing*. Vienna, Austria: R Foundation for Statistical Computing.
  39. Norell MA, Clark JM. 1990 A reanalysis of *Bernissartia fagesii*, with comments on its phylogenetic position and its bearing on the origin and diagnosis of the Eusuchia. *Bull. Inst. R. Sci. Nat. Belg.* **60**, 115–128.
  40. Ronquist F *et al.* 2012 MrBayes 3.2: efficient Bayesian phylogenetic inference and model choice across a large model space. *Syst. Biol.* **61**, 539–542. (doi:10.1093/sysbio/sys029)
  41. Goloboff PA, Farris JS, Nixon KC. 2008 TNT, a free program for phylogenetic analysis. *Cladistics* **24**, 774–786. (doi:10.1111/j.1096-0031.2008.00217.x)
  42. Goloboff PA, Catalano SA. 2016 TNT version 1.5, including a full implementation of phylogenetic morphometrics. *Cladistics* **32**, 221–238. (doi:10.1111/cla.12160)
  43. Benton MJ, Clark JM. 1988 Archosaur phylogeny and the relationships of the Crocodylia. In *The phylogeny and classification of the tetrapods*, vol. 1 (ed. MJ Benton), pp. 295–338. Oxford, UK: Clarendon Press.
  44. Brochu CA. 2003 Phylogenetic approaches toward crocodylian history. *Annu. Rev. Earth Planet. Sci.* **31**, 357–397. (doi:10.1146/annurev.earth.31.100901.141308)
  45. Brochu CA. 1996 Closure of neurocentral sutures during crocodylian ontogeny: implications for maturity assessment in fossil archosaurs. *J. Vertebr. Paleontol.* **16**, 49–62. (doi:10.1080/02724634.1996.10011283)
  46. Ikejiri T. 2012 Histology-based morphology of the neurocentral synchondrosis in *Alligator mississippiensis* (Archosauria, Crocodylia). *Anat. Rec.* **295**, 18–31. (doi:10.1002/ar.21495)
  47. Olsen SL. 1988 The identification of stone and metal tool marks on bone artifacts. In *Scanning electron microscopy in archaeology* (ed. SE Olsen), pp. 337–360. New York, NY: Oxford University Press.
  48. Greenfield HJ. 2004 The butchered animal bone remains from Ashqelon, Afridar—area G. *Antiqot* **45**, 243–261.
  49. Zeng Z. 1980 The period of the killing off of the elephant, crocodile, and peacock in the adjacent regions of the Pearl River delta. *J. South China Norm. Univ. (Nat. Sci. Ed.)* 173–185.
  50. Bapst DW. 2012 Paleotree: an R package for paleontological and phylogenetic analyses of evolution. *Methods Ecol. Evol.* **3**, 803–807. (doi:10.1111/j.2041-210X.2012.00223.x)
  51. Martin JE, Buffetaut E, Naksri W, Lauprasert K, Claude J. 2012 *Gavialis* from the Pleistocene of Thailand and its relevance for drainage connections from India to Java. *PLoS ONE* **7**, e44541. (doi:10.1371/journal.pone.0044541)
  52. Martin BGH, Bellairs AD. 1977 The narial excrescence and pterygoid bulla of the gharial, *Gavialis gangeticus* (Crocodylia). *J. Zool. London* **182**, 541–558. (doi:10.1111/j.1469-7998.1977.tb04169.x)
  53. Martin JE. 2019 The taxonomic content of the genus *Gavialis* from the Siwalik Hills of India and Pakistan. *Pap. Palaeontol.* **5**, 483–497. (doi:10.1002/spp2.1247)
  54. Iijima M *et al.* 2020 Taxonomic overview of Neogene crocodylians in Myanmar. *J. Vertebr. Paleontol.* **40**, e1879100. (doi:10.1080/02724634.2021.1879100)
  55. Lull RS. 1944 Fossil *Gavialis* from North India. *Am. J. Sci.* **242**, 417–430. (doi:10.2475/ajs.242.8.417)
  56. Müller L. 1927 Ergebnisse der Forschungsreisen Prof. E. Stromers in den Wüsten Ägyptens. V. Tertiäre Wirbeltiere: 1. Beiträge zur Kenntnis der Krokodilier des ägyptischen Tertiärs. *Abh. Bayer. Akad. Wiss.* **31**, 1–97. (doi:10.1515/9783486756135)
  57. Salas-Gismondi R, Moreno-Bernal JW, Scheyer TM, Sánchez-Villagra MR, Jaramillo C. 2019 New Miocene Caribbean gavialoids and patterns of longirostry in crocodylians. *J. Syst. Palaeontol.* **17**, 1049–1075. (doi:10.1080/14772019.2018.1495275)
  58. Salas-Gismondi R, Flynn JJ, Baby P, Tejada-Lara JV, Claude J, Antoine P-O. 2016 A new 13 million year old gavialoid crocodylian from proto-Amazonian mega-wetlands reveals parallel evolutionary trends in skull shape linked to longirostry. *PLoS ONE* **11**, e0152453. (doi:10.1371/journal.pone.0152453)
  59. Riff D, Aguilera OA. 2008 The world’s largest gharials *Gryposuchus*: description of *G. croizati* n. sp. (Crocodylia, Gavialidae) from the Upper Miocene Urumaco Formation, Venezuela. *Paläontol. Z.* **82**, 178–195. (doi:10.1007/BF02988408)
  60. Gold MEL, Brochu CA, Norell MA. 2014 An expanded combined evidence approach to the *Gavialis* problem using geometric morphometric data from crocodylian braincases and Eustachian systems. *PLoS ONE* **9**, e105793. (doi:10.1371/journal.pone.0105793)



61. Norell MA. 1988 Cladistic approaches to evolution and paleobiology as applied to the phylogeny of alligatorids. Ph.D. thesis, Yale University, New Haven, CT.
62. Brochu CA. 1997 Phylogenetic systematics and taxonomy of Crocodylia. Ph.D. thesis, University of Texas, Austin, TX.
63. Brochu CA, Gingerich PD. 2000 New tomistomine crocodylian from the Middle Eocene (Bartonian) of Wadi Hitan, Fayum Province, Egypt. *Contrib. Mus. Paleontol. Univ. Mich.* **30**, 251–268.
64. Hone D, Mallon JC, Hennessey P, Witmer LM. 2020 Ontogeny of a sexually selected structure in an extant archosaur *Gavialis gangeticus* (Pseudosuchia: Crocodylia) with implications for sexual dimorphism in dinosaurs. *PeerJ* **8**, e9134. (doi:10.7717/peerj.9134)
65. Reber SA, Nishimura T, Janisch J, Robertson M, Fitch WT. 2015 A Chinese alligator in heliox: formant frequencies in a crocodylian. *J. Exp. Biol.* **218**, 2442–2447. (doi:10.1242/jeb.119552)
66. Reber SA, Janisch J, Torregrosa K, Darlington J, Vliet KA, Fitch WT. 2017 Formants provide honest acoustic cues to body size in American alligators. *Sci. Rep.* **7**, 1816. (doi:10.1038/s41598-017-01948-1)
67. Fitch WT, Hauser MD. 2003 Unpacking 'honesty': vertebrate vocal production and the evolution of acoustic signals. In *Acoustic communication* (eds RR Fay, AN Popper), pp. 65–137. New York, NY: Springer.
68. Reby D, McComb K. 2003 Anatomical constraints generate honesty: acoustic cues to age and weight in the roars of red deer stags. *Anim. Behav.* **65**, 519–530. (doi:10.1006/anbe.2003.2078)
69. Weishampel DB. 1981 Acoustic analyses of potential vocalization in lambeosaurine dinosaurs. *Paleobiology* **7**, 252–261. (doi:10.1017/S0094837300004036)
70. Fitch WT. 1999 Acoustic exaggeration of size in birds via tracheal elongation: comparative and theoretical analyses. *J. Zool.* **248**, 31–48. (doi:10.1017/S095283699900504X)
71. Lydekker R. 1886 Siwalik Crocodylia, Lacertilia, & Ophidia. *Palaeontol. Indica* **3**, 209–240.
72. Hecht MK, Malone B. 1972 On the early history of the gavialid crocodylians. *Herpetologica* **28**, 281–284.
73. Norell MA, Storrs GW. 1989 Catalogue and review of the type fossil crocodylians in the Yale Peabody Museum. *Postilla* **203**, 1–28.
74. Head J. 2001 Systematics and body size of the gigantic, enigmatic crocodyloid *Rhamphosuchus crassidens*, and the faunal history of Siwalik Group (Miocene) crocodylians. *J. Vertebr. Paleontol.* **21**, 59A. (doi:10.1671/0272-4634(2001)021[0392:AROTPP]2.0.CO;2)
75. Garrick LD, Lang JW. 1977 Social signals and behaviors of adult alligators and crocodiles. *Am. Zool.* **17**, 225–239. (doi:10.1093/icb/17.1.225)
76. Dinets V. 2013 Long-distance signaling in crocodylia. *Copeia* 517–526. (doi:10.1643/CE-12-125)
77. Qian Y. 2009 A preliminary study of the battle-axes using institution in ancient China. *Acta Archaeol. Sin.* 1–34.
78. Yang Y. 1997 Shenzhen ji linjing diqu xian Qin qingtongqi zhuzao jishu de kaocha (a study of pre-Qin bronze casting techniques in Shenzhen and surrounding region). *Kaogu* 87–96.
79. Li Y. 2001 Guangdong caoqi qingtong shidai yicun shulue (an outline of early Bronze age remains in Guangdong). *Kaogu* 57–65.
80. Higham C, Higham T, Ciarla R, Douka K, Kijngam A, Rispoli F. 2011 The origins of the Bronze age of southeast Asia. *J. World Prehistory* **24**, 227–274. (doi:10.1007/s10963-011-9054-6)
81. Wen H, Xu J, Huang Z, He Y. 1980 The preliminary analysis of the distribution and the cause of change of *Crocodylus porosus* of China in the historical periods. *J. Shanghai Norm. Univ. (Nat. Sci.)* **3**, 109–121.
82. Zeng J. 1974 Lun ji zhong dianxing redai dongwu zai nanfang miejue de shiqi (Timing of extinction of typical tropical fauna in the south). *J. South China Norm. Univ. (Nat. Sci. Ed.)* 92–96.
83. Huang C, Zeng T, Ye F, Xie L, Wang Z, Wei G, Lo L, Deng W, Rao Z. 2018 Natural and anthropogenic impacts on environmental changes over the past 7500 years based on the multi-proxy study of shelf sediments in the northern South China Sea. *Quat. Sci. Rev.* **197**, 35–48. (doi:10.1016/j.quascirev.2018.08.005)
84. Teng SN, Xu C, Teng L, Svenning JC. 2020 Long-term effects of cultural filtering on megafauna species distributions across China. *Proc. Natl Acad. Sci. USA* **117**, 486–493. (doi:10.1073/pnas.1909896116)
85. Lorenzen ED *et al.* 2011 Species-specific responses of Late Quaternary megafauna to climate and humans. *Nature* **479**, 359–364. (doi:10.1038/nature10574)
86. Li X, Jiang G, Tian H, Xu L, Yan C, Wang Z, Wei F, Zhang Z. 2015 Human impact and climate cooling caused range contraction of large mammals in China over the past two millennia. *Ecography* **38**, 74–82. (doi:10.1111/ecog.00795)
87. Bartlett LJ, Williams DR, Prescott GW, Balmford A, Green RE, Eriksson A, Valdes PJ, Singarayer JS, Manica A. 2016 Robustness despite uncertainty: regional climate data reveal the dominant role of humans in explaining global extinctions of Late Quaternary megafauna. *Ecography* **39**, 152–161. (doi:10.1111/ecog.01566)
88. Iijima M, Qiao Y, Lin W, Peng Y, Yoneda M, Liu J. 2022 An intermediate crocodylian linking two extant gharials from the Bronze Age of China and its human-induced extinction. FigShare.